Vision-Based Calibration Study for Structural Displacement Measurement

Felipe J. Perez[a], **Dat V. Nguyen**[b], **and Omar E. Mora**[c]

California State Polytechnic University, Pomona 3801 West Temple Ave., Pomona, CA, U.S.A.
E-mail: [a]*fperez@cpp.edu,* [b]*datvnguyen@cpp.edu,* [c]*oemora@cpp.edu*

Current structural displacement measurements require the use of instrumentation such as linear variable differential transformers (LVDT's), dashpots, extensometers, accelerometers or similar devices. These instruments require careful calibration, installation, and a data acquisition system, which may be cost prohibitive in some cases. Furthermore, when conducting experiments on countertop-sized structures, these displacement measuring devices interfere with the response of the specimen by virtue of their attachments to the specimen. This paper considers a remote vision-based system for experimental static displacement measurements of structures. The system requires a digital camera, a tripod, and a computer vision algorithm. Since the measurements are remote, this method is ideal for experimental measurements of small structures, but is also applicable to larger structures. To test and evaluate the performance of the proposed method, 14 tests were performed by varying the focal length and the distance to target by obtaining distance measurements using a calibrated meter stick. In total, 225 distances were measured. Results show that the error in a distance measurement decreases to 0% as the measured distance increases for a fixed focal length. The error in a 1 mm distance measurement decreases to within 1% as the focal length increases for a distance to object of 2 m. Therefore, the proposed methodology is recommended for efficiently measuring static displacements.

Keywords: Computer vision, Structural Health Monitoring, Displacement Measurement

1. Introduction

In the last decade, advancements in structural health monitoring (SHM) have resulted in improved spatial and temporal resolution, efficiency, and cost-effectiveness (Fukuda et al., 2010; Fukuda et al. 2013; Ribeiro et al., 2014; Gentile and Bernardini, 2010). The most common method for SHM is the use of sensors, both contact (Linear Variable Differential Transformer (LVDT), accelerometer, etc.) and non-contact (laser vibrometer, Light Detection and Ranging (LIDAR), etc.) types (Feng et al., 2015). However, contact methods can be time-consuming and expensive due to the complex installation scheme of the sensors and their data acquisition systems (Feng et al., 2015). One of the most important parameters in SHM is structural displacement measurement because not only does it help assess a structure's condition and

Advancements in Civil Engineering for a Sustainable, Equitable, and Resilient Infrastructure
Edited by Felipe J. Perez, Siamak Yazdani, Omar E. Mora, and Yasser Salem

ISBN: 978-981-18-5185-8; doi: 10.3850/978-981-18-5185-8_62-40-1

performance, but also provides vital information regarding maintenance to maximize its operational lifespan (Ye et al., 2013). To eliminate the need for sensors to be physically attached to a structure, a noncontact vision-based system is needed. This is particularly useful when structures are small, such as in a laboratory or classroom setting, where demonstrations of structural response are required, but attached instrumentation impacts the response.

The experimental study presented herein is an extension of previous work by Perez and Mora (2022). The experiments are set up to obtain measurements between two points on a calibrated meter stick by analyzing images taken from a camera. While the study performed by Perez and Mora (2022) provides promising results with an observed percent error within 1.15% for a 1 mm measurement when the camera is placed 1 meter away from the meter stick, the present study tests the flexibility in placement of the camera by increasing the distance up to 4 meters.

2. Methodology

The proposed methodology consists of the following items: a structure, an image acquisition system (a digital camera and a zoom lens), software for processing the images, targets mounted on the structure for tracking of movement, a computer, and a computer vision algorithm (software) to measure the displacements. Figure 1 shows the proposed setup and Figure 2 shows the approach for measuring displacements within a Region of Interest (ROI) on a structure. First, a camera is affixed to a tripod at a specified distance to structure. The structure is equipped with targets for tracking displacements. An image is captured prior to loading the structure, followed by an image after loading.

Referring to Figure 2, the pixel coordinates of the target in the first frame are acquired using an image processing software. In this frame, the structure

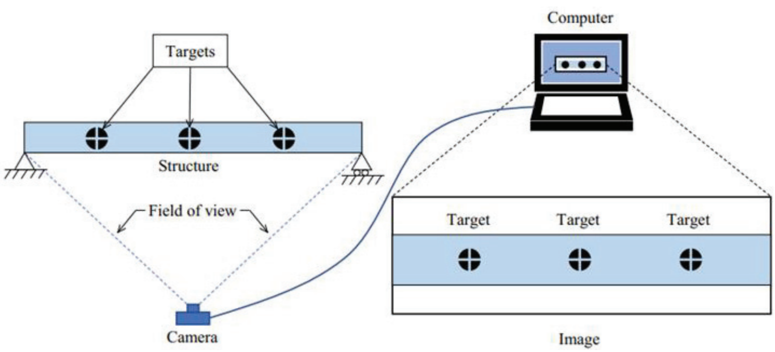

Figure 1. Proposed vision-based structural displacement measurement setup (Perez and Mora, 2022).

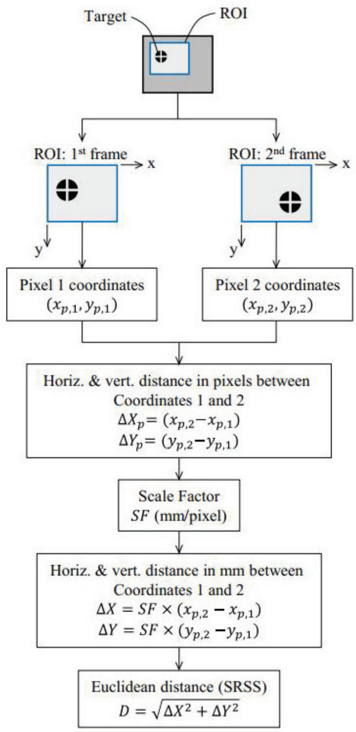

Figure 2. Proposed vision-based sensing methodology (Perez and Mora, 2022).

is unloaded, so the target is in its original, undeformed position. Once the structure is loaded, the pixel coordinates of the same target are identified in the second frame. Next, the horizontal and vertical distances are measured in pixels using the acquired coordinates in those two frames. These distances are then converted from pixels to millimeters by applying a scale factor using Eq. 1 as follows:

$$SF = \frac{d_{\text{object}}}{d_{\text{image}}} \left[\frac{mm}{\text{pixel}} \right] \tag{1}$$

where, d_{object} = physical dimension of an object (mm)
d_{image} = image dimension of an object (pixel)

Lastly, the vertical and horizontal distances in millimeters are converted to a Euclidean distance using the Square Root of the Sum of Squares (SRSS).

3. Description of Experiments

To determine the efficacy of the proposed method in measuring structural displacement remotely via a vision-based system, multiple calibration experiments were carried out in this study. The methodology described above was

Table 1. Test summary.

Distance to	Focal Length (mm)						
Object (m)	9.5	19	31	38	72	104	167
2	Test 1	Test 2	Test 3	Test 4	Test 5	Test 6	Test 7
4	Test 8	Test 9	Test 10	Test 11	Test 12	Test 13	Test 14

slightly adjusted as follows. Instead of using a physically loaded structure, a meter stick was positioned on a countertop, where the marks on the meter stick are used to represent the impact of a moving target on a structure. This was done for the reason that a calibrated meter stick represents the ground truth for the intended measurements and eliminates any errors associated with an experimental setup and instrument calibration. Therefore, instead of using two different frames as shown in Figure 2, the pixel coordinates of two different tick marks on the calibrated meter stick were acquired using a single frame.

The camera used in this study is a Sony DSC-RX10M4 with a Zeiss Vario-Sonnar T* f/2.4-4 zoom lens. The camera was positioned at distances of 2 m and 4 m from the meter stick. The center of the lens was aligned with the center of the meter stick. For each distance to object, seven different focal lengths were considered by adjusting the camera's zoom setting. As the camera was zoomed closer to the object, the focal length increased. All photographs were taken using a remote-control shutter to avoid moving the camera. Each test provided one image, which was then processed using a program called IrfanView. In total, there were 14 tests performed (two distances to object with seven focal lengths), as summarized in Table 1.

Each image taken had a width of 5472 pixels and a height of 3648 pixels. As the focal length increased, a smaller portion of the meter stick was captured in the image. As a result, the field of view was reduced. For each test, multiple displacement measurements were taken across the portion of the meter stick that was in view. While Tests 1 and 8 had the widest field of view, Tests 7 and 14 had the narrowest field of view due to the greatest zoom setting in the camera. As a result, Tests 1 and 8 allowed for more measurements than Tests 7 and 14.

4. Results and Discussion

A total of 225 distance measurements were taken in this experimental study. All the measurements and their respective percentage errors are summarized in Tables 2 and 3.

Table 2. Summary of test results with a 2-meter distance to object.

	Test 1		Test 2		Test 3		Test 4		Test 5		Test 6		Test 7	
Actual Dist. (mm)	Meas. (mm)	Error (%)	Meas. (mm)	Error (%)	Meas. (mm)	Error (%)	Meas. (mm)	Error (%)	Meas. (mm)	Error (%)	Meas. (mm)	Error (%)	Meas. (mm)	Error (%)
1	0.750	24.96	1.26	25.56	0.94	5.86	1.01	0.76	0.96	3.95	0.99	0.84	1.01	0.91
5	5.002	0.05	5.27	5.47	4.95	0.95	5.04	0.79	4.93	1.45	4.96	0.84	5.01	0.15
30	30.01	0.05	30.14	0.45	30.03	0.08	30.10	0.34	29.91	0.31	29.94	0.21	30.01	0.05
50	50.02	0.05	50.48	0.95	50.14	0.29	50.00	0.00	49.89	0.22	49.96	0.08	50.07	0.15
60	59.53	0.78	60.52	0.87	60.20	0.34	60.08	0.13	59.88	0.20	59.92	0.13	60.00	0.00
70	70.03	0.05	70.57	0.81	70.11	0.16	70.03	0.04	69.80	0.28	69.93	0.10	70.02	0.02
90	89.54	0.51	90.41	0.45	90.23	0.26	89.92	0.08	89.85	0.16	89.95	0.05	88.03	2.19
100	100.05	0.05	100.45	0.45	100.14	0.14	100.00	0.00	99.85	0.15	100.06	0.06	100.00	0.00
200	200.10	0.05	200.65	0.33	200.12	0.06	200.00	0.00	200.17	0.09	200.12	0.06	–	–
220	220.11	0.05	220.49	0.22	220.24	0.11	220.03	0.01	220.15	0.07	220.00	0.00	–	–
300	300.15	0.05	300.85	0.28	300.41	0.14	300.25	0.08	300.02	0.01	–	–	–	–
320	319.66	0.11	320.69	0.22	320.53	0.16	320.28	0.09	320.00	0.00	–	–	–	–
400	399.70	0.07	400.80	0.20	400.70	0.17	400.38	0.09	–	–	–	–	–	–
500	500.25	0.05	500.75	0.15	500.83	0.17	500.25	0.05	–	–	–	–	–	–
520	520.26	0.05	520.59	0.11	520.80	0.15	520.15	0.03	–	–	–	–	–	–
600	599.80	0.03	600.70	0.12	600.66	0.11	600.00	0.00	–	–	–	–	–	–
700	699.85	0.02	700.40	0.06	700.48	0.07	–	–	–	–	–	–	–	–
800	799.90	0.01	800.35	0.04	800.00	0.00	–	–	–	–	–	–	–	–
900	899.95	0.01	900.31	0.03	–	–	–	–	–	–	–	–	–	–
1000	1000.0	0.00	1000.0	0.00	–	–	–	–	–	–	–	–	–	–

Table 3. Summary of test results with a 4-meter distance to object.

	Test 8		Test 9		Test 10		Test 11		Test 12		Test 13		Test 14	
Actual Dist. (mm)	Meas. (mm)	Error (%)	Meas. (mm)	Error (%)	Meas. (mm)	Error (%)	Meas. (mm)	Error (%)	Meas. (mm)	Error (%)	Meas. (mm)	Error (%)	Meas. (mm)	Error (%)
1	1.46	45.64	0.51	48.64	0.93	7.46	1.05	5.13	0.93	6.92	1.00	0.25	0.96	4.32
5	5.18	3.50	5.14	2.72	4.94	1.30	4.85	2.98	4.92	1.60	5.01	0.25	5.07	1.34
30	29.87	0.45	30.30	1.01	30.23	0.76	30.34	1.14	30.05	0.18	30.08	0.25	30.17	0.56
50	50.46	0.93	50.34	0.67	50.59	1.17	50.23	0.46	50.13	0.27	50.03	0.07	50.26	0.53
60	60.76	1.27	60.61	1.01	60.46	0.76	60.43	0.71	60.11	0.18	60.06	0.10	60.34	0.56
70	70.03	0.04	70.88	1.25	70.33	0.47	70.37	0.53	70.21	0.30	70.08	0.12	70.36	0.51
90	90.63	0.70	90.91	1.01	90.68	0.76	90.52	0.57	90.29	0.33	90.13	0.15	90.39	0.44
100	100.93	0.93	100.67	0.67	100.56	0.56	100.46	0.46	100.27	0.27	100.16	0.16	100.41	0.41
200	200.82	0.41	200.82	0.41	201.11	0.56	201.17	0.59	200.53	0.27	200.32	0.16	200.43	0.22
220	220.39	0.18	221.37	0.62	221.16	0.53	221.06	0.48	221.28	0.58	220.28	0.13	220.41	0.19
300	301.75	0.58	301.49	0.50	301.36	0.45	301.38	0.46	300.80	0.27	300.30	0.10	300.00	0.00
320	321.32	0.41	321.52	0.48	321.41	0.44	321.52	0.47	320.88	0.27	320.35	0.11	–	–
400	401.65	0.41	401.64	0.41	401.60	0.40	401.58	0.40	400.93	0.23	400.00	0.00	–	–
500	501.54	0.31	501.28	0.26	501.54	0.31	501.79	0.36	500.93	0.19	–	–	–	–
520	521.11	0.21	521.32	0.25	521.59	0.31	521.67	0.32	520.88	0.17	–	–	–	–
600	601.44	0.24	601.44	0.24	601.48	0.25	601.73	0.29	600.53	0.09	–	–	–	–
700	701.34	0.19	701.08	0.15	701.42	0.20	701.43	0.20	700.00	0.00	–	–	–	–
800	800.21	0.03	801.23	0.15	801.05	0.13	801.12	0.14	–	–	–	–	–	–
900	901.13	0.13	900.87	0.10	900.68	0.08	900.56	0.06	–	–	–	–	–	–
1000	1000.0	0.00	1000.0	0.00	1000.0	0.00	1000.0	0.00	–	–	–	–	–	–

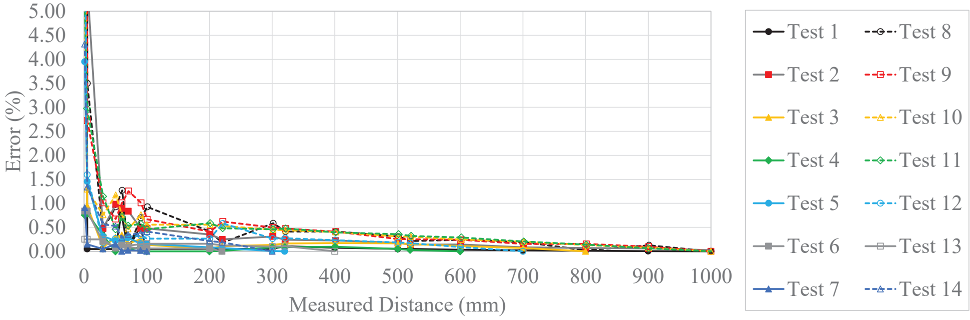

Figure 3. Error in distance measurements for all tests with a 2-m and a 4-m distance to object.

The relationship between the percent error and the measured distance is shown in Figure 3. For tests with a shorter focal length, the error is large (e.g., 48.64% for Test 9 at a 1 mm measurement) since the resolution for the image is quite poor. Thus, the y-axis in Figure 3 is truncated at 5% so that the data presented is more clearly visible. Referring to Figure 3, as a general trend, for a given focal length, the error in a distance measurement reduces for larger measurement magnitudes. For all tests, Tables 2 and 3 show that the error in a distance measurement decreases to 0% as the measured distance increases for a fixed focal length. Furthermore, Figure 3 and Tables 2 and 3 show that smaller errors are observed for the 2-m distance to object (Tests 1 to 7) compared with the 4-m distance to object (Tests 8 to14). Tables 2 and 3 also show that tests with the smallest focal lengths (e.g., Tests 1, 2, 8, and 9) resulted in greater measurement errors, while tests with greater focal lengths (e.g., Tests 6, 7, 13, and 14) resulted in the smallest measurement errors. Thus, the error tends to decrease as the focal length increases.

Table 2 shows that a 1 mm measurement was achieved with an error less than 5% for Tests 4, 5, 6, and 7. Similarly, Table 3 shows that a 1 mm measurement was achieved with an error less than 5% for Tests 13 and 14. This means that a 1 mm resolution is achievable within a 5% error for a 2-m distance to object with a minimum focal length of 38 mm (See Test 4 in Table 1). Similarly, a 1-mm resolution is achievable within a 5% error for a 4-m distance to object with a minimum focal length of 104 mm (See Test 13 in Table 1).

5. Conclusions

This paper studies a new structural displacement measurement method using a vision-based system and a computer vision algorithm. The following conclusions can be drawn from this study: (1) The error in a distance measurement decreases to 0% as the measured distance increases for a fixed focal length for a distance to target of 2 m and 4 m; (2) Smaller distance measurement errors are observed for a 2-m distance to object compared to a 4-m distance to object; (3) The error in a distance measurement decreases as the focal length increases; (4) The minimum focal lengths required to achieve a 1 mm resolution in a displacement measurement within a 5% error for a 2-m distance to object and a 4-m distance to object are 38 mm and 104 mm, respectively; (5) The proposed methodology is recommended for efficiently measuring structural displacements ranging from 1 mm to 1000 mm at distance to object of 2 m and 4 m, with appropriate adjustments in focal length.

Acknowledgment

The authors thank the Special Projects for Improving the Classroom Experience (SPICE) Program at California State Polytechnic University, Pomona for funding the equipment utilized in this study.

References

Feng, D., Feng, M.Q., Ozer, E. and Fukuda, Y. (2015). A vision-based sensor for noncontact structural displacement measurement. *Sensors, 15*(7), pp. 16557–16575.

Fukuda, Y., Feng, M.Q., Narita, Y., Kaneko, S.I. and Tanaka, T. (2013). Vision-based displacement sensor for monitoring dynamic response using robust object search algorithm. *IEEE Sensors Journal, 13*(2), pp. 4725–4732.

Fukuda, Y., Feng, M.Q. and Shinozuka, M. (2010). Cost-effective vision-based system for monitoring dynamic response of civil engineering structures. *Structural Control and Health Monitoring, 17*(8), pp. 918–936.

Gentile, C. and Bernardini, G. (2010). An interferometric radar for non-contact measurement of deflections on civil engineering structures: laboratory and full-scale tests. *Structure and Infrastructure Engineering, 6*(5), pp. 521–534.

Perez, F.J. and Mora, O.E. (2022). A Vision-Based System for Structural Displacement Measurement, in 7th *World Congress on Civil, Structural, and Environmental Engineering*, ICEPTP 127-1 to 127-8. Virtual Conference, April 10–12, 2022.

Ribeiro, D., Calcada, R., Ferreira, J. and Martins, T. (2014). Non-contact measurement of the dynamic displacement of railway bridges using an advanced video-based system. *Engineering Structures, 75*, pp. 164–180.

Ye, X.W., Ni, Y.Q. and Yin, J.H. (2013). Safety monitoring of railway tunnel construction using FBG sensing technology. *Advances in Structural Engineering, 16*(8), pp. 1401–1409.